Photocatalytic Properties of Porous Metal Oxide Networks Formed by Nanoparticle Infiltration in a Polymer Gel Template

Dmitry G. Shchukin,† Jan H. Schattka, Markus Antonietti, and Rachel A. Caruso*

Max Planck Institute of Colloids and Interfaces, D-14424 Potsdam, Germany, and Physico-Chemical Research Institute, 220050 Minsk, Belarus

Received: September 6, 2002

The infiltration of preformed nanoparticles in a porous polymer gel template for the formation of inorganic networks retaining high porosity is described. The use of a number of metal oxide sols including titania, zirconia, and indium oxide, and mixtures of TiO_2/ZrO_2 and TiO_2/In_2O_3, resulted in structures that demonstrated templating of the initial organic gel. The final networks were homogeneously porous and had significant surface areas of up to 65 $m^2\ g^{-1}$. The wall thickness of the inorganic structure and the surface area, along with the final amount of inorganic material that infiltrated the polymer gel, were found to be dependent on the metal oxide being considered. Photocatalytic studies of the titania-containing networks were monitored by the degradation of 2-chlorophenol and compared with the reference titania photocatalyst, Degussa P25. The titania network was about 20% more active than the standard and the mixed metal oxides showed higher activity again (up to 80% more active than the Degussa P25 sample). The addition of the second metal oxide to the titania decreased the amount of the rutile crystalline phase in the final structure and increased the network surface area, both of these changes are considered positive for enhancement of the photocatalytic activity.

Introduction

The contamination of water with halogenated aromatics, such as the carcinogenic chlorophenols, is an important ecological issue. A solution to this problem is the photocatalytic purification of industrial wastewaters employing photochemically active semiconductors as photocatalysts. This mode of purification is promising as it gives the possibility of complete mineralization of the harmful organics, resulting in CO_2 and H_2O as final products.[1,2] A number of reviews have been published during the last 15 years in which different environmental applications and mechanisms of heterogeneous photocatalytic processes have been described.[3−5] It has been established that titanium dioxide is currently the best photocatalytic material among other semiconductors, as it possesses extremely high photocorrosion stability and activity of the photogenerated holes.[1]

However, high photocatalytic activity of heterogeneous photocatalysts requires large surface area of the photocatalytic material, and therefore, colloidal solutions of nanosized particles are often used in the photocatalytic reactor. This leads to a considerable problem: the separation of the photocatalytic nanoparticles from the treated solution after irradiation.[4] One approach to overcoming this problem is the use of large photocatalytically active particles (>100 nm in diameter) possessing an intrinsic porous structure and, as a result, high surface area despite the larger overall particle diameter, that can be more easily separated from the solution.

Templating procedures are an ideal way to control material structure: The morphology of the final material, including outer dimensions and shape, along with inner structuring such as pore systems and their size distributions can be predetermined by selection of the template. In some cases, this procedure requires a defined mold, which acts as a scaffold around which the desired material is built, thereby forming a cast or inverse structure of the mold. The final material can be either an inverse replica or a hollow replica, depending on whether a complete cast or a coating was achieved during the templating process.[6] For the formation of porous materials in materials science, templating techniques have been shown to afford uniform pore sizes on a number of scales: macro, meso, and micro.[7−9] The structure of the pores is dependent on the form of the initial template (for example, spherical (latex templates) or cylindrical (amphiphilic block copolymer porogens) pores can be produced[10,11]), and the final porosity of the material is dictated by the template. This ability to regulate porosity and pore structure is being used frequently to obtain materials with required properties, which enhance efficiencies in final applications. For example, controlling the pore and overall material structures can increase surface areas.

Inorganic structures are commonly templated with organic materials, which are easily removed with solvent or heating procedures. A template that has proved useful for the formation of macroporous materials is the porous polymer gel.[12−15] The template itself can easily be prepared and the preparation method allows flexibility in the porous structure, pH stability, and functionality of the polymer gel.[16,17] The polymer gels have been studied as templates for the formation of titania and zirconia porous structures using a sol−gel synthesis route within the polymer gel pores, hereafter referred to as the precursor templating method.[12−14] This involved soaking the porous material in a metal oxide precursor solution followed by hydrolysis and condensation reactions, resulting in an amorphous inorganic coating on the polymer scaffold. Removal of the polymer by pyrolysis at 500 °C left highly porous crystalline titania or zirconia networks with significant surface areas, which

* Corresponding author. Fax: +49 331 567 9502. E-mail: Rachel.Caruso@mpikg-golm.mpg.de.
† Physico-Chemical Research Institute.

10.1021/jp026929i CCC: $25.00
Published on Web 01/04/2003

were influenced by the choice of the initial polymer gel structure.[12−14]

Proposed applications for these porous materials include catalysis and photocatalysis. The precursor-formed titania structures have been assessed for catalytic abilities with the photodecomposition of salicylic acid and 2-chlorophenol photodegradation.[14] It was found that mixing the titania/zirconia precursors gave final porous materials with enhanced photocatalytic activity at certain Ti:Zr ratios. This was attributed to the presence of zirconia inhibiting the anatase-to-rutile phase transition, resulting in higher surface areas of the mixed metal oxide material, and the ability of zirconia to act as an adsorbent in the vicinity of the photocatalytic material.[14] It has been shown previously that the photocatalytic properties of titania can be combined with the properties of redox-stable inorganic oxides (such as SiO_2,[18,19] ZrO_2,[20] or Al_2O_3[21]), which allows one to regulate the final surface area, the ratio of anatase to rutile phase titania crystals, the surface acidity, plus the overall adsorption and hydrophilic properties of the resulting composite photocatalyst. Thus the combination of two metal oxides makes it possible to tune materials for specific reactions so that higher yields can be achieved.

Preformed iron oxide (10 nm particles of magnetite) and titanium dioxide (8 nm particles of anatase) nanoparticles have been incorporated into "sponge-like", 2-hydroxyethyl methacrylate/acrylic acid polymer gels by Breulmann et al.[15] Infiltration times of 24 h or 7 weeks were used for the iron oxide and titania, respectively. On removal of the polymer gel, porous inorganic structures were obtained.[15] It is difficult to distinguish from the images shown whether a coating or casting procedure was obtained for these materials. However, the templating mechanism is described as a physical confinement of the nanoparticles in the template, which swells in solution and shrinks on drying.

In this paper, the formation of porous metal oxide and mixed metal oxide structures using the templating of a glycidyl methacrylate/acrylamide polymer gel and preformed metal oxide nanoparticles is described. The metal oxides include titania, zirconia, indium oxide, and combinations of the latter two oxides with titania. The soaking time used here is substantially shorter, soaking for two weeks was sufficient to produce porous structures, than that documented previously for the titanium dioxide structures (7 weeks).[15] The photocatalytic activity of titanium dioxide and the mixed oxide (titania and either zirconia or indium oxide) networks were compared with that of commercial Degussa P25, a commonly used titania reference catalyst, by monitoring the photodegradation of 2-chlorophenol.

Experimental Section

Materials. The surfactant used during the synthesis of the porous polymer gel was Tween 60 (T60, polyoxyethylene (20) sorbitan monostearate). The monomers acrylamide (AA) and glycidyl methacrylate (GMA), along with the cross-linker ethylene glycol dimethacrylate (EGDMA), and the initiator potassium persulfate (KPS) were used for polymer synthesis. For the preparation of the TiO_2 and In_2O_3 sols the precursors $TiCl_4$ and $In(NO_3)_3{\cdot}5H_2O$ were utilized. All these chemicals were purchased from Aldrich. $ZrO(NO_3)_2$ was used as the precursor for the preparation of the ZrO_2 sol. This precursor along with HNO_3 and a 25% aqueous solution of ammonia were obtained from Fluka.

All chemicals were used as received. The water used in all experiments was obtained from a three-stage Millipore Milli-Q Plus 185 purification system and had a resistivity higher than 18 MΩ cm.

Template (Polymer Gel) Formation. The preparation of the polymer gel used here as a template has previously been reported,[14] and is as follows: The structure directing surfactant (25.00 g of Tween 60) and water (50.00 mL) were combined with stirring before the monomers (6.26 g AA and 6.26 g GMA) and cross-linker (2.51 g) were added. Stirring continued until a homogeneous, though turbid, solution was obtained. Following the addition of the initiator (0.63 g), the mixture was transferred into test tubes that were placed in an oil bath at 55 °C for a period of 15 h, where polymerization occurred. The gel was cut into disks and washed with water several times before soxhlet extraction was conducted (ethanol, 2 days) to remove the surfactant. Further washing with water was performed until the conductivity of the water in which the polymer gel pellets were soaking no longer changed.

Sol Synthesis. Three metal oxide colloids (TiO_2, In_2O_3, and ZrO_2) were utilized in this work. The preparation procedure for all of the metal oxide sols was the same and follows a method published previously:[22] Initially, the inorganic precursor (0.027 mol) was dissolved in 0.5 M aqueous HCl (20 mL). The precursor was hydrolyzed by the addition of a 12.5 wt % aqueous ammonia solution (6−15 mL, this is dependent on the metal) while the solution was vigorously stirred at 0 °C. It is important in this step that the pH value of the final solution does not exceed 5−6. The metal oxide precipitate was then washed up to 10 times with water and centrifugation/decantation cycles until a turbid supernatant solution was obtained. The metal oxide was then redispersed by the addition of a stabilizer (concentrated nitric acid, 1 mol HNO_3 per 5 mol of metal) and ultrasonic treatment (10 min in a Transsonic Digitals bath sonifier). The sols were dialyzed against Milli-Q water using a Spectra/Por membrane (MWCO: 6−8000) to adjust the pH to a value between 3 and 5. Ready-to-use colloid suspensions had concentrations of 5.1 wt % (TiO_2), 6.0 wt % (In_2O_3), and 5.4 wt % (ZrO_2), and an average diameter of 4 nm for TiO_2 (containing anatase crystals), 6 and 10 nm for the In_2O_3 and ZrO_2 particles, respectively. The latter two samples were X-ray amorphous.

Templating Procedure. For the impregnation of inorganic particles into the organic template the dry gel (see drying procedure below) was immersed in the aqueous colloidal solutions or mixtures (TiO_2/In_2O_3 or TiO_2/ZrO_2 with Ti:In or Ti:Zr ratios of 1:1 by weight) and stored at room temperature in the dark for a set period. After initial trial soaking periods of 2.5 to 14 days for the titania sol a period of 2 weeks was chosen for the immersion time of all samples as good reproducibility, and less shrinkage and cracks were obtained in the final inorganic material. The polymer/inorganic oxide composite was then washed with water for 5 min, dried for 4 h at 60 °C, and calcined at 450 °C (with a ramp rate of 10 °C min^{-1}) for 2 h in flowing air.

Characterization. To dry the polymer gel sample for templating and electron microscopy viewing, a Critical Point Dryer, CPD 030 from BAL-TEC, was used. The polymer gel was initially exchanged from the solvents water to ethanol, and then to acetone (a method known to suppress drying artifacts).[23] Scanning electron microscopy (SEM) (Zeiss DSM 940 instrument) was used to examine both the original gel structure and that of the resulting inorganic networks. The samples were broken to expose fresh surfaces and mounted onto carbon-coated stubs before sputter coating. To view the nanoparticles composing the walls of the network structure the samples were set in LR-White resin, and then ultrathin sections (30 to 100 nm in thickness) were obtained using a Leica ultracut UCT ultra-

microtome. Carbon or non-coated copper grids were used to support the thin sections. A Zeiss EM 912 Omega transmission electron microscope (TEM) was employed for analysis of the finer details of the local structure. Estimation of the average diameter of the colloid particles in solution was performed using static light scattering (Specord M40 spectrophotometer equipped with light-scattering chamber).

To determine the weight percent of inorganic to organic material in the intermediate stages of the templating process, thermogravimetric analysis was conducted using a Netzsch TG 209 apparatus. A Micromeritics Gemini II 2375 Surface Area Analyzer was used to obtain the specific surface area from BET (Brunauer−Emmett−Teller) analysis after N_2 adsorption. The crystal structure of the metal oxide systems was determined from wide-angle X-ray scattering (WAXS), Enraf-Nonius PDS-120. A Perkin-Elmer AAnalyst 700 atomic absorbance spectrometer was employed to measure the metal oxide ratios in the mixed metal oxide networks.

Photocatalytic Activity Measurements. The photodecomposition of 2-chlorophenol was monitored to determine the photocatalytic activity of the titania-based metal oxide networks. The photochemical reactor was a cylindrical flask of ca. 90 mL with a bottom quartz window (3.6 cm in diameter) equipped with a magnetic stirring bar and filters (IR-vis and UV) so that light within $340 < \lambda < 500$ nm was transmitted. Illumination was provided by a high-pressure mercury lamp (Philips HPK 125 W). The total radiant flux was 10 mW cm^{-2}. For the irradiation experiments, 40 mL of the continuously stirred 2-chlorophenol solution (10^{-3} M, pH = 4.5) containing the photocatalyst (2 g L^{-1}) was used. To allow sufficient adsorption of 2-chlorophenol on the surface of the photocatalyst, the 2-chlorophenol solution was stirred in the dark for 2 h before the irradiation. Prior to the experiment, the metal oxide networks were broken into small pieces of greater than 100 nm in diameter. Commercial titania, Degussa P25, was employed as a reference material. The concentration of 2-chlorophenol was determined by HPLC using an LDC/Milton Roy system, which was comprised of a Constametric 3000 isocratic pump and a Spectro Monitor D UV-detector adjusted to 254 nm. A reverse-phase column (4.6 mm internal diameter and 25 cm long) packed with Spherisorb 5 0DS2 was used. The mobile phase was a mixture of methanol (35%), deionized doubly distilled water (55%), and acetonitrile. Identification of the eluting compounds was made by comparing their retention times with those of commercial compounds purchased from Aldrich.

Results and Discussion

Materials employed as templates should possess an interesting structure, be stable during the templating procedure, and be removable to obtain the final inorganic network. The template used here is a polymer gel prepared in the presence of the surfactant Tween 60. It has a globular structure, seen in the SEM image in Figure 1a. It is porous and the structure is homogeneous throughout the gel. The specific surface area of the dried polymer, obtained from BET analysis, is 27 m^2 g^{-1}. As the gel is composed of acrylamide and glycidyl methacrylate, cross-linked with EGDMA, it was stable during the templating processes, which involved soaking in aqueous sol solutions with pH values between 3 and 5, washing in water to dislodge excess nanoparticles on the outer surface, followed by drying. Note that the glycidyl groups of this gel are almost completely hydrolyzed to two chelating hydroxy-groups, which promote the very good binding of the oxophilic peptized nanoparticles. Slight swelling and shrinkage of the gel occurred during these procedures, but the characteristic structure was maintained. The immersion time of the polymer gel in the sol was set to 2 weeks after analyzing the final materials obtained by soaking polymer gels in the titania sol for periods of 2.5 to 14 days. Immersion times less than 2 weeks gave porous structures, however there was substantial shrinkage (∼ 50%) and cracks in the final inorganic material, which was regarded as insufficient coating. The polymeric template was removed by heating the hybrid material to 450 °C in the presence of oxygen, which resulted in pyrolysis of the organic scaffold.

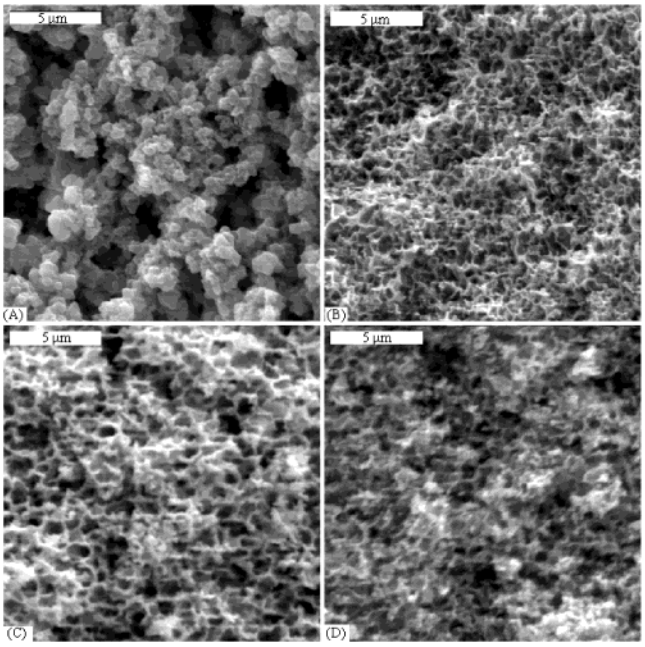

Figure 1. SEM images of (a) the initial template, a T60 polymer gel; and the template formed inorganic networks: (b) TiO_2, (c) In_2O_3, and (d) TiO_2/In_2O_3.

SEM images of the final inorganic materials are shown in Figure 1b−d. Homogeneous porous inorganic networks were achieved for the oxides examined as well as their mixtures with titania (TiO_2/In_2O_3 and TiO_2/ZrO_2). These networks show resemblance to the polymer gel template. The mechanism by which these structures are formed is proposed to be as follows: While the polymer gel was soaking in the sol, nanoparticles entered the pores where adsorption of the nanoparticles to the polymer occurred. As the water was removed from the pores on drying, the nanoparticles from the sol deposited on the polymer walls, resulting in a coating of the template. Long-term storage of a metal oxide-loaded polymer template in water led to desorption of the metal oxide particles, as they were found to leach into the solution. Compared to the initial template, the final structures obtained after calcination showed considerable shrinkage (∼15−25%). This shrinkage is comparable to that obtained using the precursor templating method.[12−14] It has been found with the templating of three-dimensional, ordered structures, such as colloidal crystals, that the use of a precursor method to form inorganic materials generally results in higher shrinkage (20 to 35%)[24,25] compared to the approach presented here, using the infiltration of preformed nanoparticles (shrinkage of 5−6%).[26] However, in the colloidal crystal example, the resulting inorganic is a cast (that is an inverse replica obtained by filling of the pores with nanoparticles). Here the pore structure of the organic template, the polymer gel, was filled with a colloidal solution (≤6 wt % metal oxide). Therefore, the pore volume was not filled with nanoparticles, resulting in

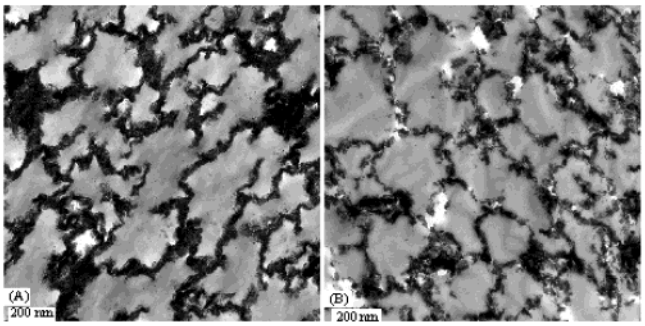

Figure 2. TEM images of ultramicrotomes of (a) the polymer gel and titania hybrid, and (b) the final TiO_2 network. The samples were set in an epoxy resin.

TABLE 1: Properties of the Inorganic Networks: Specific Surface Area (SA) Obtained from BET Analysis of N_2 Adsorption Measurements, Final Weight Percent of Inorganic Material Remaining on Removal of the Organic Template Obtained from TGA of the Hybrid Structures, and TiO_2 Content in the Mixed Metal Oxide Materials Derived from AAS Measurements

material	SA ($m^2\ g^{-1}$)	wt % inorganic	TiO_2 content (wt %)
T60 polymer gel	27	0	0
TiO_2	45	18	100
ZrO_2	50	9	0
In_2O_3	53	35	0
TiO_2/ZrO_2	65	17	67
TiO_2/In_2O_3	63	24	58

a coating of the template and a related shrinkage during drying and calcination.

The diameter of the pores produced after removing the templates for the different oxide networks lies between 400 and 700 nm. The inorganic wall thickness, as estimated from TEM images, varies within the range of 50−150 nm, depending on the metal oxide. Thicker walls were observed for In_2O_3, TiO_2, and the mixed metal oxide samples. The zirconia network, on the other hand, formed the most brittle structure with relatively thin walls (∼50 nm). Such deviations in the wall thickness could be explained by the differences in the initial nanoparticles. First, the zirconia particles are substantially larger, with a diameter of 10 nm, than the titania and indium oxide particles (4 and 6 nm, respectively). Also from the data obtained using TGA (Table 1), a much lower weight percent of the inorganic material in the hybrid structures is seen for the zirconia sample, indicating less infiltration and adhesion of the zirconia nanoparticles onto the gel carrying hydroxy-functional groups. A comparison can also be made to the initial templating with nanoparticle work where 7-week impregnation time was used to obtain stable titania structures as the final product when using 8-nm-sized TiO_2 nanoparticles.[15] Hence, variation in the wall thickness is most likely due to the particle diameter, its infiltration behavior, and the template/nanoparticle attractive interactions.

The nanoparticles making up the network structures can be seen using TEM. In Figure 2, the polymer gel/TiO_2 composite and the final titania material are depicted as microtomed thin slices of the samples. Again, shrinkage can be observed when comparing the two TEM images. Patches of nanoparticles, along with the ribbon-like arrangement, are due to the position of the ultramicrotome cut through the sample. The ribbon-like structure of the nanoparticles reflects the coating of the polymer gel.

TEM images of the ultramicrotomed samples indicate that the porous structure of the metal oxide networks obtained here is similar to the structures reported previously for the networks prepared by the precursor templating method[14] and by using preformed particles.[15] However, the SEM images of the samples under consideration look different from those prepared using the precursor method, as they appear to show a more uniform distribution of pore sizes. This is believed to be due to the preparation of the network for SEM analysis: The more brittle material yields a flatter breaking plane, which offers less spatial information, but allows a more representative view of the pore structure.

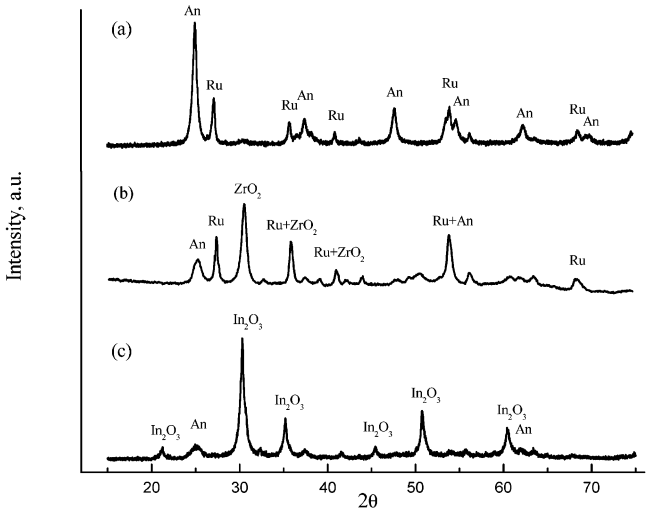

Figure 3. Wide-angle X-ray scattering spectra of the final network materials composed of (a) TiO_2, (b) TiO_2/ZrO_2, and (c) TiO_2/In_2O_3. (An) and (Ru) signify the phase modifications of anatase and rutile titania, respectively.

The BET surface area of the inorganic materials obtained after calcination is tabulated (Table 1). The inorganic materials have higher specific surface areas than the initial organic template, and the values were dependent on the type of nanoparticle impregnated in the template. The surface areas of the mixed metal oxides were higher again. Comparing these values with those obtained with the precursor templating method indicates that similar or higher surface areas can be obtained for the single metal oxides using the preformed particles, e.g., 45 and 50 $m^2\ g^{-1}$ for preformed titania and zirconia, respectively, compared with 31 and 48 $m^2\ g^{-1}$ for the same metal oxides obtained using precursor and sol−gel chemistry.[14] However, such comparisons have to be made carefully as the calcination programs were not identical, nor has either technique been systematically optimized. The mixed titania/zirconia material with a similar Ti-to-Zr ratio obtained using a mixture of the precursors for templating was amorphous,[14] while the use of preformed nanoparticles allowed the formation of a crystalline metal oxide network composed of two discrete metal oxides as observed from X-ray diffraction.

The X-ray diffraction data (see Figure 3) revealed the presence of both anatase and rutile phases in the titania network with the ratio between them being approximately equal to that of the initial TiO_2 sol annealed under similar conditions (∼15 wt % rutile). The mixing of zirconia and especially indium oxide with titania made the titanium dioxide more stable against the anatase-to-rutile phase transformation,[4,5,22] which usually begins in pure TiO_2 between 450 and 500 °C,[22] and also inhibited the crystallite growth upon heat treatment (This is seen by broadening of the peaks corresponding to the anatase modification for the TiO_2/In_2O_3 and TiO_2/ZrO_2 networks, Figure 3). The scattering peaks from In_2O_3 and ZrO_2 can be attributed to the cubic modification of indium oxide and the monoclinic modification of zirconia. Annealing the initial In_2O_3 and ZrO_2 sols (without

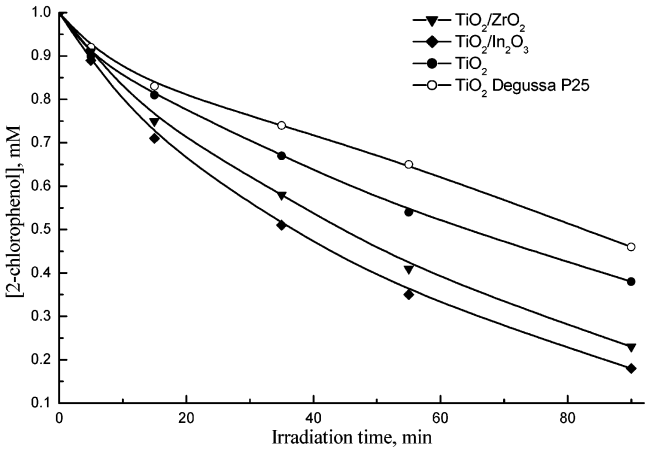

Figure 4. 2-Chlorophenol photodegradation in the presence of the photocatalysts: Degussa P25, and the template formed networks TiO_2, TiO_2/ZrO_2, and TiO_2/In_2O_3. Plotted as the 2-chlorophenol concentration against illumination time.

the template) under the same conditions resulted in the formation of the same crystal phases.

The degradation of 2-chlorophenol was chosen to assess the photocatalytic activity of the inorganic materials. The overall photocatalytic degradation reaction of 2-chlorophenol is as follows:

$$ClC_6H_4OH + {}^{13}/_{2}O_2 \xrightarrow{h\nu,\ TiO_2} [\text{intermediates}] \xrightarrow{h\nu\ TiO_2} 6CO_2 + HCl + 2H_2O$$

The photocatalytic experiments for the different titania-based templated structures, as well as the reference photocatalyst (Degussa P25), were carried out under the same conditions: pH value, initial 2-chlorophenol concentration, and temperature. The photocatalytic activity was monitored by the decrease in the 2-chlorophenol concentration as a function of time (Figure 4). All the materials under investigation (TiO_2, TiO_2/ZrO_2, and TiO_2/In_2O_3) were efficient, with half of the 2-chlorophenol degraded within 35 and 90 min of irradiation. The reproducibility of these data was good, with an error limit below 6%.

The porous titania material prepared by the templating method showed a 20% increase in photocatalytic activity compared to the Degussa P25 titania, as observed in Figure 4. The addition of the second metal oxide component leads to a further considerable increase in the photocatalytic activity. This is most pronounced for the TiO_2/In_2O_3 photocatalyst, which showed an 80% increase in the 2-chlorophenol decomposition compared to the Degussa P25 titania (Figure 4). As Degussa P25 is a technically optimized product these results are significant.

The specific surface area of the titania network and the Degussa P25 are the same (see Table 1, specific surface area for the Degussa P25 is 45 $m^2\ g^{-1}$),[14] hence the improved photocatalytic activity of the porous titania material was ascribed to the high photochemical as well as photoelectrochemical activity of the initial TiO_2 sol, which has been shown to have a low level of surface recombination of photogenerated charges.[22] The use of sol−gel reactions with titanium(IV) isopropoxide in the templating procedure (instead of the prepared colloid solution) produced porous titania structures with a photocatalytic activity that is lower than the activity of Degussa P25 (65%).[14] This could be attributed in part to the differences in surface area of the titania samples, and different surface properties are expected to be important factors.

The mixed metal oxides have an increased surface area compared with the single oxides, (see Table 1) and improved photocatalytic activity (Figure 4). This increased activity not only results from the increased surface area, as the presence of the second metal oxide can also contribute in different ways. The second metal oxide, as it was emphasized above, makes titanium dioxide more stable against the anatase-to-rutile phase transformation, thereby increasing the amount of the more photoactive titania form, anatase, in the final material.[4,5] Thus, an increased photocatalytic activity would be expected for the mixed oxide materials. Another reason for the enhanced activity is the surface interaction between the second metal oxide and titania.[20,27] It is well-known that the activity of pure TiO_2 depends greatly on the density and acidity of the surface hydroxyl groups.[28,29] Mixing of TiO_2 with ZrO_2 or In_2O_3 makes the surface hydroxyl groups more acidic, possibly while heating,[30] resulting in improved adsorption of the decomposing substance on the surface of the mixed metal oxide materials. As studies have shown that such improved adsorption increases the probability of radical attack,[18] the mixed metal oxides would again be more active than the titania material.

The best photocatalytic activity among the materials explored was the TiO_2/In_2O_3 system. The arguments just discussed are valid for this mixed oxide network, however another important point is believed to contribute to this enhancement of activity. It has been shown that an acceleration of the spatial electron/hole pair separation can occur due to transfer of the photogenerated electron from the TiO_2 surface to the In_2O_3,[31] which is then followed by the reduction of oxygen on the In_2O_3 surface. Hence the mixed oxide material containing In_2O_3 was most photocatalytically active, presumably due to this very efficient separation of the charge carriers.

Conclusions

The combined use of polymer templates and preformed metal oxide nanoparticles has been shown to successfully generate porous metal oxide networks with high structural definition for a number of systems: titania, zirconia, indium oxide, and the mixtures of titania/zirconia and titania/indium oxide. The infiltration times were relatively short compared to previously published results. The surface areas of the final inorganic networks were found to increase when two metal oxide sols were combined for the templating procedure.

The titania-containing structures showed excellent photocatalytic activity, with efficiencies better than the Degussa P25 titania (which is the bench mark due to its high activity). The presence of the second metal oxide (zirconia or indium oxide) in the titania structure leads to an increase in the materials specific surface area, and a decrease in the formation of the rutile phase of titania, leaving the more photocatalytically active anatase phase. Therefore, an increased overall photocatalytical activity resulted. The possibility of increased surface acidity and decreased charge recombination were also factors discussed to explain the increased activity of the mixed metal oxide materials.

Acknowledgment. The Max Planck Society is acknowledged for financial support. D.G.S. acknowledges the German Academic Exchange Service (DAAD) for a one-year research scholarship (No. A/01/10817). Rona Pitschke is thanked for ultramicrotoming the samples and for transmission electron microscopy analysis. We are grateful to Degussa Hüls for supplying the P25 titania sample.

References and Notes

(1) van Well, M.; Dillert, R. H. G.; Bahnemann, D. W. *TiO_2-based Environmental Photocatalysis in Solar Engineering*; *American Society of Mechanical Engineers*, 1996.
(2) Theurich, J.; Lindner, M.; Bahnemann, D. W. *Langmuir* **1996**, *12*, 6368−6376.
(3) Fox, M. A.; Dulay, M. T. *Chem. Rev.* **1993**, *93*, 341−357.
(4) Legrini, O.; Oliveros, E.; Braun, A. M. *Chem. Rev.* **1993**, *93*, 671−698.
(5) Hoffmann, M. R.; Martin, S. T.; Choi, W.; Bahnemann, D. W. *Chem. Rev.* **1995**, *95*, 69−96.
(6) Caruso R. A. In *Topics in Current Chemistry: Colloid Chemistry*; Antonietti, M., Ed.; Springer-Verlag: Heidelberg, in press.
(7) Caruso, R. A.; Antonietti, M. *Chem. Mater.* **2001**, *13*, 3272−3282.
(8) Göltner, C. G.; Antonietti, M. *Adv. Mater.* **1997**, *9*, 431.
(9) Gies, H.; Marler, B. *Zeolites* **1992**, *12*, 42.
(10) Holland, B. T.; Blanford, C. F.; Stein, A. *Science* **1998**, *281*, 538−540.
(11) Göltner, C. G.; Berton, B.; Krämer, E.; Antonietti, M. *Adv. Mater.* **1999**, *11*, 395−398.
(12) Caruso, R. A.; Giersig, M.; Willig, F.; Antonietti, M. *Langmuir* **1998**, *14*, 6333−6336.
(13) Caruso, R. A.; Antonietti, M.; Giersig, M.; Hentze, H.-P.; Jia, J. *Chem. Mater.* **2001**, *13*, 1114−1123.
(14) Schattka, J. H.; Shchukin, D. G.; Jia, J.; Antonietti, M.; Caruso, R. A. *Chem. Mater.*, in press.
(15) Breulmann, M.; Davis, S. A.; Mann, S.; Hentze, H.-P.; Antonietti, M. *Adv. Mater.* **2000**, *12*, 502−507.
(16) Antonietti, M.; Göltner, C.; Hentze, H.-P. *Langmuir* **1998**, *14*, 2670.
(17) Antonietti, M.; Caruso, R. A.; Göltner, C. G.; Weissenberger, M. C. *Macromolecules* **1999**, *32*, 1383−1389.
(18) Anderson, C.; Bard, A. J. *J. Phys. Chem.* **1995**, *99*, 9882−9885.
(19) Tada, H.; Akazawa, M.; Kubo, Y.; Ito, S. *J. Phys. Chem. B* **1998**, *102*, 6360−6366.
(20) Fu, X.; Clark, L. A.; Yang, Q.; Anderson, M. A. *Environ. Sci. Technol.* **1996**, *30*, 647−653.
(21) Anderson, C.; Bard, A. J. *J. Phys. Chem. B* **1997**, *101*, 2611−2616.
(22) Poznyak, S. K.; Kokorin, A. I.; Kulak, A. I. *J. Electroanal. Chem.* **1998**, *442*, 99−105.
(23) Reimer, L.; Pfefferkorn, G. *Scanning Electron Microscopy*; Springer: Berlin, 1972.
(24) Velev, O. D.; Jede, T. A.; Lobo, R. F.; Lenhoff, A. M. *Chem. Mater.* **1998**, *10*, 3597.
(25) Blanford, C. F.; Yan, H.; Schroden, R. C.; Al-Daous, M.; Stein, A. *Adv. Mater.* **2001**, *13*, 401−407.
(26) Subramania, G.; Constant, K.; Biswas, R.; Sigalas, M. M.; Ho, K.-M. *Appl. Phys. Lett.* **1999**, *74*, 3933.
(27) Anderson, R.; Mountjoy, G.; Smith, M. E.; Newport, R. J. *J. Non-Cryst. Solids* **1998**, *232−234*, 72−79.
(28) Papp, J.; Soled, S.; Dwight, K.; Wold, A. *Chem. Mater.* **1994**, *6*, 496−500.
(29) Shibata, K.; Kiyoura, T.; Kitagawa, J.; Sumiyoshi, T.; Tanabe, K. *Bull. Chem. Soc. Jpn.* **1973**, *46*, 2985−2989.
(30) Kung, H. *Transition Metal Oxides: Surface Chemistry and Catalysis*; Elsevier: New York, 1991.
(31) Poznyak, S. K.; Talapin, D. V.; Kulak, A. I. *J. Phys. Chem. B* **2001**, *105*, 4816−4823.